Molecular Vision 2017; 23:823-831 <http://www.molvis.org/molvis/v23/823>
Received 30 March 2017 | Accepted 22 November 2017 | Published 24 November 2017

Antiangiogenic effect of dasatinib in murine models of oxygen-induced retinopathy and laser-induced choroidal neovascularization

Songyi Seo, Wonhee Suh

College of Pharmacy, Chung-Ang University, Seoul, Korea

Purpose: Vascular endothelial growth factor (VEGF) is a principal mediator of pathological ocular neovascularization, which is the leading cause of blindness in various ocular diseases. As Src, a non-receptor tyrosine kinase, has been implicated as one of the major signaling molecules in VEGF-mediated neovascularization, the present study aimed to investigate whether dasatinib, a potent Src kinase inhibitor, could suppress pathological ocular neovascularization in murine models of oxygen-induced retinopathy (OIR) and choroidal neovascularization (CNV).

Methods: Tube formation, scratch wounding migration, and cell proliferation assays were performed to measure the inhibitory effect of dasatinib on VEGF-induced angiogenesis in human retinal microvascular endothelial cells. Murine models of OIR and laser-induced CNV were used to assess the preventive effect of an intravitreal injection of dasatinib on pathological neovascularization in the retina and choroid. Neovascularization and Src phosphorylation were evaluated with immunofluorescence staining.

Results: Dasatinib efficiently inhibited VEGF-induced endothelial proliferation, wounding migration, and tube formation. In mice with OIR and laser injury-induced CNV, eyes treated with a single intravitreal injection of dasatinib exhibited significant decreases in pathological neovascularization compared with that of controls injected with vehicle. The dasatinib-treated OIR mice also showed a decrease in Src phosphorylation in the periretinal tufts. The intravitreal injection of dasatinib did not cause ocular toxicity at the treatment dose administered.

Conclusions: These results demonstrated that dasatinib suppressed pathological neovascularization in the mouse retina and choroid. Therefore, dasatinib may be indicated for the treatment of ischemia-induced proliferative retinopathy and neovascular age-related macular degeneration.

The formation of new blood vessels is not only crucial to many physiologic processes but is also fundamental to the pathogenesis of various diseases. In particular, excessive formation of abnormal blood vasculature is considered a leading cause of vision impairment and irreversible blindness in various ocular diseases. In retinopathy of prematurity (ROP) and proliferative diabetic retinopathy (PDR), retinal hypoxia resulting from vaso-obliteration, insufficient vascular growth, and hyperglycemia have been identified as major triggers for pathological neovascularization. The upregulation of hypoxia-inducible proangiogenic factors induces the excessive growth of leaky retinal vasculature, which leads to vitreous hemorrhage, retinal detachment, and severe vision loss. Pathological neovascularization also occurs in subretinal and choroidal tissue in patients with neovascular age-related macular degeneration (AMD). Abnormalities or defects in Bruch's membrane induce hypoxia, oxidative stress, and inflammation, which disturb the balance of pro- and anti-angiogenic factors in the direction of angiogenesis. The outgrowth of fragile and leaky neovessels originating from the choroidal vasculature in the subretinal area leads to the detachment of the RPE from the choroid, fibrotic scarring, and permanently diminished vision. Among the numerous factors that have been identified to stimulate pathological ocular neovascularization, vascular endothelial growth factor (VEGF) is the most prominent mediator. Many previous studies have indicated that the expression level of VEGF is strongly associated with the severity of ocular neovascularization in patients with PDR, ROP, and neovascular AMD [1-4]. Moreover, anti-VEGF agents have shown substantial therapeutic efficacy in preventing disease progression and in improving visual acuity in patients with neovascular AMD [5,6].

VEGF activates VEGF receptor 2 (VEGFR2) in endothelial cells and initiates multiple intracellular signaling cascades involved in cell proliferation, migration, morphogenesis, and permeability. Among the various VEGF-induced signal transduction molecules, Src, a non-receptor tyrosine kinase, is a key component in angiogenic signaling cascades. Eliceiri and colleagues demonstrated that Src kinase activity was required for VEGF-mediated angiogenesis in chick embryos

Correspondence to: Wonhee Suh, College of Pharmacy, Chung-Ang University, Seoul 06974, Korea, Phone: 82-2-820-5960; FAX: 82-2-816-7338; email: wsuh@cau.ac.kr

and mice [7]. Other researchers reported that Src mediated VEGF-induced endothelial cell migration and antiapoptotic activity via activation of focal adhesion kinase [8]. Given the importance of VEGF in pathological ocular neovascularization and the critical role of Src in VEGF angiogenic signaling pathways, attenuating VEGF-induced angiogenesis with Src inhibitors may be a sound therapeutic strategy to regulate excessive neovascularization in diverse ocular diseases.

Therefore, we proposed that dasatinib, a small-molecule Src kinase inhibitor approved by the USA Food and Drug Administration for the treatment of leukemia and renal cell carcinoma, would show therapeutic effects in pathological ocular neovascularization. In our previous study, we demonstrated that dasatinib efficiently blocked VEGF-induced Src phosphorylation and prevented VEGF- and diabetes-induced breakdown of the blood–retinal barrier [9]. In the present study, we aim to determine the antiangiogenic effects of dasatinib in murine models of oxygen-induced retinopathy (OIR) and laser-induced choroidal neovascularization (CNV), which mimic ROP and neovascular AMD, respectively.

METHODS

Cell culture: Human retinal microvascular endothelial cells (HRMECs), endothelial growth medium-2 (EGM-2), and endothelial basal medium (EBM) were purchased from Lonza (Walkersville, MD). The HRMECs were plated in gelatin-coated plates and cultured in EGM-2 at 37 °C in a humidified atmosphere of 5% CO_2 in air. The HRMECs used for the experiments were between passages 3 and 6.

In vitro angiogenesis assays: The tube formation assay was performed by seeding cells (3×10^4/well) in 24-well plates coated with Matrigel (BD Bioscience, Bedford, MA) and cultured in EBM containing 1% fetal bovine serum (FBS, Lonza) in the absence or presence of 100 ng/ml recombinant human VEGF (rhVEGF; R&D Systems, Minneapolis, MN) and 25 nM dasatinib (Selleckchem, Houston, TX). After a 6-h incubation period, tube lengths were measured in four random microscope fields.

For the scratch wounding migration assay, confluent cell monolayers grown in gelatin-coated four-well plates were scratched using a micropipette tip. The plates were washed with PBS (1X; 137 mM NaCl, 2.7 mM KCl, 10 mM Na_2HPO_4, 1.5 mM KH_2PO_4; pH 7.4) to remove dislodged cells and media, and incubated with EBM containing 1% FBS in the absence or presence of rhVEGF (100 ng/ml) and dasatinib (25 nM). After a 24-h incubation period, the plates were observed using optical microscopy, and cell migration was assessed by measuring the area covered by cells that had migrated from the wound edges.

For the cell proliferation assay, cells (1×10^4/well) were seeded in gelatin-coated 96-well plates and incubated with EBM containing 1% FBS in the absence or presence of rhVEGF (100 ng/ml) and dasatinib (25 nM) for 3 days. Cell proliferation was assessed using the Cell Counting Kit-8 (CCK-8; Dojindo Molecular Technology, Rockville, MD) assay in accordance with the manufacturer's protocol. To determine the number of viable cells, the optical density of each well was read at a wavelength of 450 nm using a microplate reader (BioTek Instruments, Seoul, Korea).

Animals: All mice were cared for in accordance with the Association for Research in Vision and Ophthalmology statement for the use of animals in ophthalmic and vision research, and the protocols were approved by the Institutional Animal Care and Use Committee. Pregnant C57BL/6J mice and 9- to 10-week-old male C57BL/6J mice (Orient, Seoul, Korea) were housed at room temperature with a 12 h:12 h light-dark cycle. The mice were anesthetized with an intraperitoneal injection of ketamine (79.5 mg/kg) and xylazine (9.1 mg/kg), and the pupils of the anesthetized mice were dilated with topical 1% tropicamide (Santen, Osaka, Japan).

Mouse model of OIR: OIR was induced in mice using the protocol reported by Smith et al. [10]. Briefly, newborn mice were reared in a hyperoxic (75% oxygen) chamber connected to an oxygen controller (ProOx P110; BioSpherix, Parish, NY) from postnatal day (P)7 to P12 (Phase I: vaso-obliteration). On P12, the mice were returned to normoxia and received a single intravitreal injection of dasatinib (1 µg in 1 µl dimethyl sulfoxide [DMSO]) or 1 µl DMSO (contralateral control). After exposure to normoxic air for 5 days (P12-P17), the mice were euthanized using carbon dioxide inhalation, and both eyes were harvested for the analysis of retinal neovascularization (Phase II; neovascularization). In Phase I, hyperoxia inhibits central vessel growth in the retina and causes significant vessel loss; in Phase II, hypoxia upregulates the expression of angiogenic factors such as VEGF, thus triggering pathological neovascularization, which reaches a maximum at P17.

Quantification of retinal neovascularization: The eyes were enucleated and fixed overnight in 4% paraformaldehyde. The retinas were isolated, cut four times from the edge to the center, soaked in blocking solution (5% BSA [BSA], 5% normal donkey serum, and 0.5% Triton X-100 in PBS), and then incubated overnight at 4 °C with Alexa Fluor® 594-conjugated *Griffonia simplicifolia* isolectin B4 (1:100 dilution; Invitrogen, Carlsbad, CA) in PBS containing 1 mM $CaCl_2$. Retinas were rinsed three times with PBS, flat-mounted on microscope slides, and embedded in fluorescent mounting medium (Dako, Carpinteria, CA). Images of the

whole-mounted retina were captured using a fluorescence microscope (Olympus, Tokyo, Japan); the exposure and gain were kept constant for all samples. In each image, the number of pixels in the preretinal neovascular tufts was determined using ImageJ software (National Institutes of Health, Bethesda, MD) and was expressed as a percentage of the number of pixels in the entire retinal area.

Mouse model of laser-induced CNV: CNV was induced by laser photocoagulation of Bruch's membrane with a Micron IV image-guided laser system (532 nm; IRIS Medical, Mountain View, CA). Briefly, 9- to 10-week-old male C57BL/6J mice were anesthetized with an intraperitoneal injection of 79.5 mg/kg ketamine and 9.1 mg/kg xylazine, and the pupils were dilated with topical 1% tropicamide (Santen). Laser photocoagulation (spot size, 75 µm; intensity, 130 mW; duration, 0.1 s) was performed with four laser burns in the 3, 6, 9, and 12 o'clock positions of the posterior pole of the fundus at equal distances from the optic nerve head. Only mice with cavitation bubbles, which indicated the disruption of Bruch's membrane, were included in the study. Immediately after CNV induction, the anesthetized mice received a single intravitreal injection of dasatinib (1 µg in 1 µl DMSO) or 1 µl DMSO (contralateral control). Two weeks later, the mice were euthanized using carbon dioxide inhalation for further analysis.

Quantification of laser-induced CNV: Anesthetized mice were perfused through the left ventricle with PBS followed by 5 mg/ml fluorescein isothiocyanate (FITC)-labeled dextran (MW=10,000 Da; Sigma, St. Louis, MO). The eyes were enucleated and fixed in a 4% paraformaldehyde solution. The anterior segment and retina were removed from the eyecup, and the remaining RPE/choroid/sclera complexes were flatmounted after four radial incisions. The dissected RPE/choroid/sclera were treated with blocking solution (5% BSA, 5% normal donkey serum, and 0.5% Triton X-100 in PBS) for 1 h at room temperature and incubated with Alexa Fluor® 594-conjugated *Griffonia simplicifolia* isolectin B4 (1:100 dilution; Invitrogen) overnight at 4 °C. The samples were washed three times with PBS and mounted sclera side down on microscope slides. Images of CNV lesions were obtained using a fluorescence microscope (Olympus), and the CNV area in each image was calculated using ImageJ software (NIH). For the analysis of CNV volumes, Z-stack images of CNV lesions were acquired with an LSM780 confocal microscope (Zeiss, Jena, Germany). The sum of the CNV area in each Z-stack layer (multiplied by 5-µm thickness) was used as the volume of the CNV lesion [11].

Retinal toxicity: Normal mice received a single intravitreal injection of dasatinib (1 µg in 1 µl in DMSO) or 1 µl DMSO (contralateral control). Two weeks later, the mice were euthanized using carbon dioxide inhalation for histological and immunohistochemical examinations. For the analysis of the retinal toxicity of dasatinib in mice with OIR or CNV, ocular sections were obtained from the mice that were prepared for the OIR and CNV experiments reported in images.

Immunohistochemistry: The eyes were enucleated, fixed, embedded in optimum cutting temperature (OCT) compound (Sakura Finetek, Torrance, CA) or paraffin, sectioned, and mounted on slides. First, the endogenous peroxidase activity in the tissues was quenched. The sections were blocked with 10% normal goat serum and were then incubated with primary immunoglobulin G (IgG) against phospho-Y416 Src (p-Y416 Src; Invitrogen) or glial fibrillary acidic protein (GFAP; Dako), followed by the appropriate fluorescent secondary IgG (Dako). Blood vasculature was visualized by costaining with Alexa Fluor® 594-conjugated *Griffonia simplicifolia* isolectin B4 (Invitrogen). Cell nuclei were stained with 4',6-diamidino-2-phenylindole (DAPI; Vector Laboratories, Burlingame, CA). The images were acquired using a fluorescence microscope (Olympus), and six to eight sections were examined per group.

Histological analysis: Hematoxylin and eosin (H&E) staining was performed on paraffin-embedded sections. Retinal thickness was assessed as the ratio of A (the distance from the ganglion cell layer to the outer edge of the inner nuclear layer) to B (the distance from the ganglion cell layer to the outer edge of the outer nuclear layer).

TUNEL assay: Terminal deoxynucleotidyl transferase dUTP nick end labeling (TUNEL) assays were performed on paraffin-embedded sections using the In Situ Cell Death Detection Kit (Roche Applied Science, Mannheim, Germany) in accordance with the manufacturer's instructions. Counterstaining for total nuclei was performed by mounting with antifading medium containing DAPI (Vector Laboratories). The positive controls were paraffin sections that were treated with DNase I (1,500 U/ml; Roche Applied Science) for 10 min at room temperature to induce DNA strand breaks. Images were obtained using a fluorescence microscope (Olympus); six to ten sections were examined per group.

Statistical analysis: All results are expressed as the mean ± standard error of the mean (SEM). Statistical significance was evaluated using an one-way ANOVA followed by Bonferroni's post hoc multiple comparison test (Figure 1) or unpaired Student *t* test (Figure 2, Figure 3, and Figure 4). A p value of less than 0.05 was considered statistically significant.

RESULTS

Dasatinib inhibits VEGF-induced increase in endothelial tube formation, scratch wounding migration, and cell proliferation: We had previously determined that dasatinib (25 nM) completely blocked the VEGF-induced phosphorylation of Src on Y416 in HRMECs. Consequently, we treated the HRMECs with this concentration of dasatinib and evaluated its inhibitory effect on VEGF-induced angiogenesis [9]. As VEGF strongly enhances a variety of coordinated events required for angiogenesis, including the proliferation, migration, and morphogenesis of endothelial cells, we conducted three in vitro angiogenesis assays: Matrigel tube formation, scratch wounding migration, and CCK-8 cell proliferation assay. As shown in Figure 1, the VEGF-induced increase in tube formation, migration, and cell proliferation in HRMECs was significantly blocked by cotreatment with dasatinib. However, treatment with dasatinib alone did not affect the basal angiogenic activity of the HRMECs. These data support the hypothesis that VEGF-induced in vitro angiogenesis is effectively inhibited by dasatinib in HRMECs.

Dasatinib reduces retinal neovascularization in mice with OIR: To investigate the beneficial effect of dasatinib on pathological retinal neovascularization, we employed a mouse model of OIR, in which retinal ischemia increases the expression of various hypoxia-inducible angiogenic factors, including VEGF. Newborn pups were exposed to hyperoxia from P7 to P12. On P12, the pups were returned to the normoxic conditions and received a single intravitreal injection of dasatinib or DMSO vehicle. On P17, the extent of neovascularization was determined by quantifying the neovascular tufts, which represent pathological retinal neovascularization (Figure 2A). As illustrated in Figure 2B,

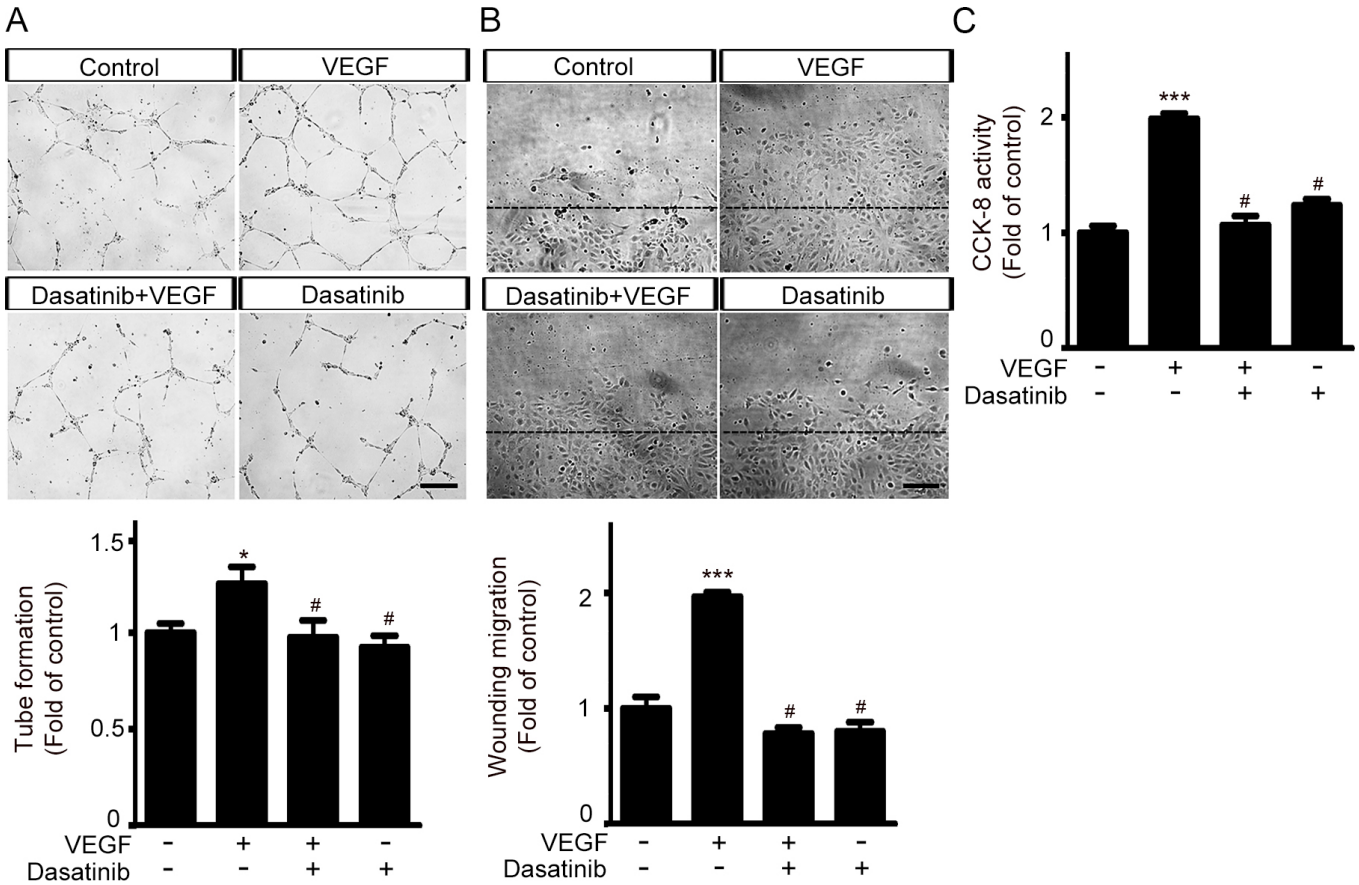

Figure 1. Dasatinib inhibits VEGF-induced increase in endothelial tube formation, scratch wounding migration, and cell proliferation. **A**: Tube formation, (**B**) scratch wounding migration, and (**C**) cell proliferation assays were performed on HRMECs in the presence or absence of rhVEGF (100 ng/ml) and dasatinib (25 nM). Tube formation, wounding migration, and cell proliferation responses were compared by normalizing the values to those of the corresponding controls. Tube formation and scratch wounding migration were quantified by measuring the tube length and the relative area covered by cells that had migrated from the wound edges (dashed black lines), respectively. Cell proliferation was assessed using the Cell-Counting Kit-8 (CCK-8) assay. Data are presented as the mean ± standard error of the mean (SEM; *p<0.05, ***p<0.001 versus control, #p<0.05 versus VEGF only, n=7, scale bars=200 µm).

the DMSO-treated control eyes had markedly high periretinal neovascularization (tuft formation). However, the periretinal neovascularization profoundly decreased in the retinas of the dasatinib-treated eyes. In the quantitative analysis, the percentage of neovascularization in the eyes treated with dasatinib and DMSO was 6.47±1.07 and 12.00±1.39 (n=6 mice per group) of the total retinal area, respectively. Thus, a single intravitreal injection of dasatinib induced a 46.08% reduction (*p<0.05) in the ischemia-induced pathological neovascularization. We also investigated whether intravitreal injection of dasatinib reduced Src phosphorylation in the retinal vasculature. In the immunohistochemical analysis of transverse retinal sections, the retinal tissues of DMSO-injected control eyes exhibited a strong staining of p-Y416 Src in isolectin B4–positive endothelial cells, whereas the retinal endothelial cells of dasatinib-injected eyes showed a substantial decrease in the p-Y416 Src signal (Figure 2C).

Dasatinib reduces CNV formation in mice with laser-induced CNV: To investigate the inhibitory effect of dasatinib on pathological CNV, we used a mouse model of laser injury-induced CNV, in which the rupture of Bruch's membrane results in

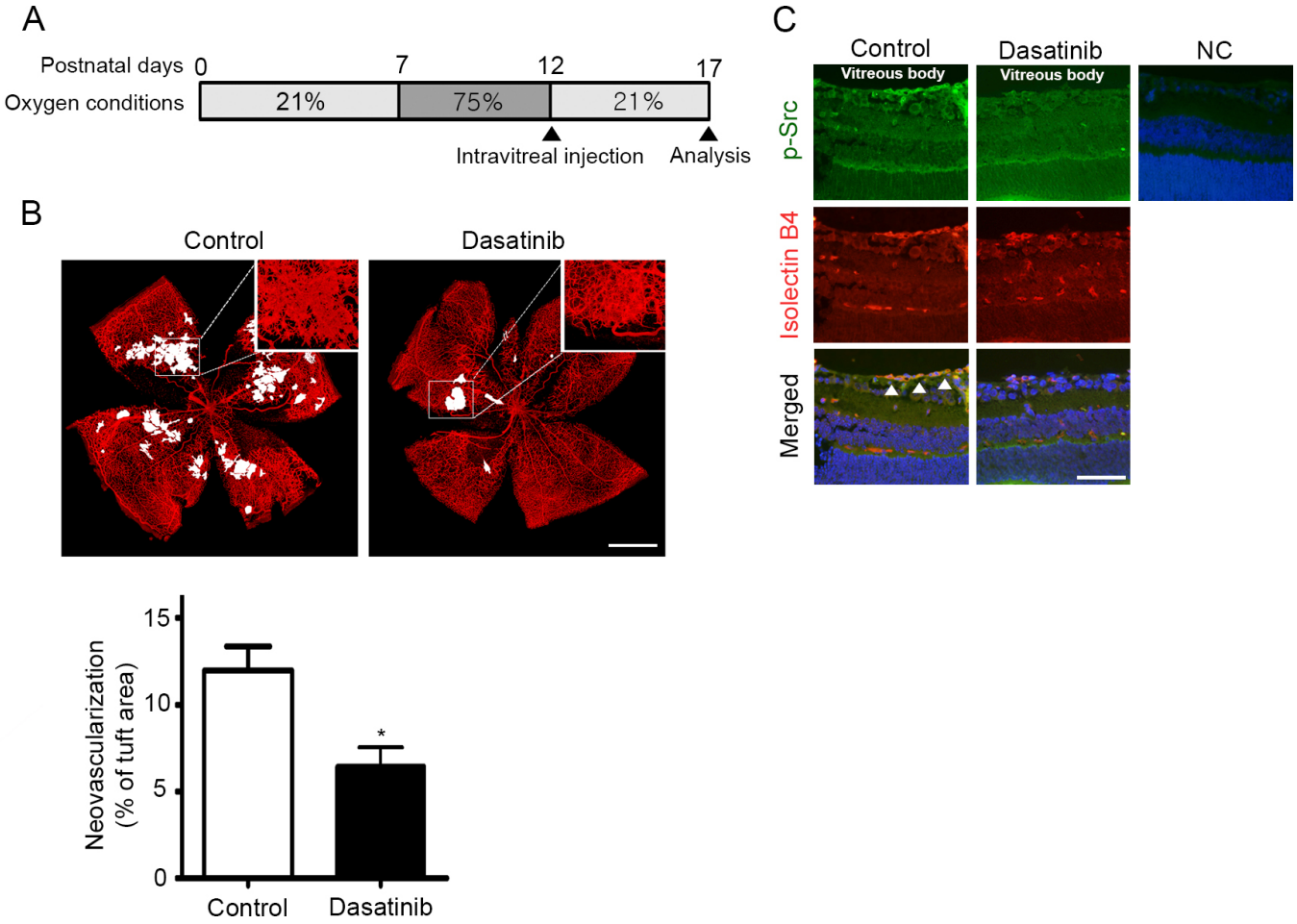

Figure 2. Dasatinib reduces retinal neovascularization in mice with OIR. **A**: Schematic diagram of the oxygen-induced retinopathy (OIR) experiment. Mice were exposed to 75% oxygen from P7 to P12, returned to normoxic conditions, and administered a single intravitreal injection of dasatinib (1 µg in 1 µl dimethyl sulfoxide [DMSO]) or DMSO (1 µl; contralateral control). On P17, the eyes were enucleated for further analysis. **B**: Representative isolectin B4–stained images of whole-mounted retinas from mice treated with DMSO (control) or dasatinib. Retinal vasculature was visualized by staining with isolectin B4 (red), and the neovascular tufts are highlighted in white. The extent of retinal neovascularization is expressed as the percentage of the number of pixels in the neovascular tuft area relative to the number of pixels in the total retinal area. All data are presented as the mean ± standard error of the mean (SEM; *p<0.05, n=6 mice per group). Scale bar=500 µm. **C**: Immunofluorescence images of p-Y416 Src and isolectin B4 of tissue sections prepared from the eyecups of mice with OIR. The arrowheads denote cells that are double-labeled with p-Y416 Src (green) and isolectin B4 (red). A section stained with irrelevant nonspecific immunoglobulin G (IgG) was included as a negative control (NC). The nuclei are shown in blue (4',6-diamidino-2-phenylindole, DAPI). Representative images were selected from three independent experiments with similar results. Scale bar=50 µm.

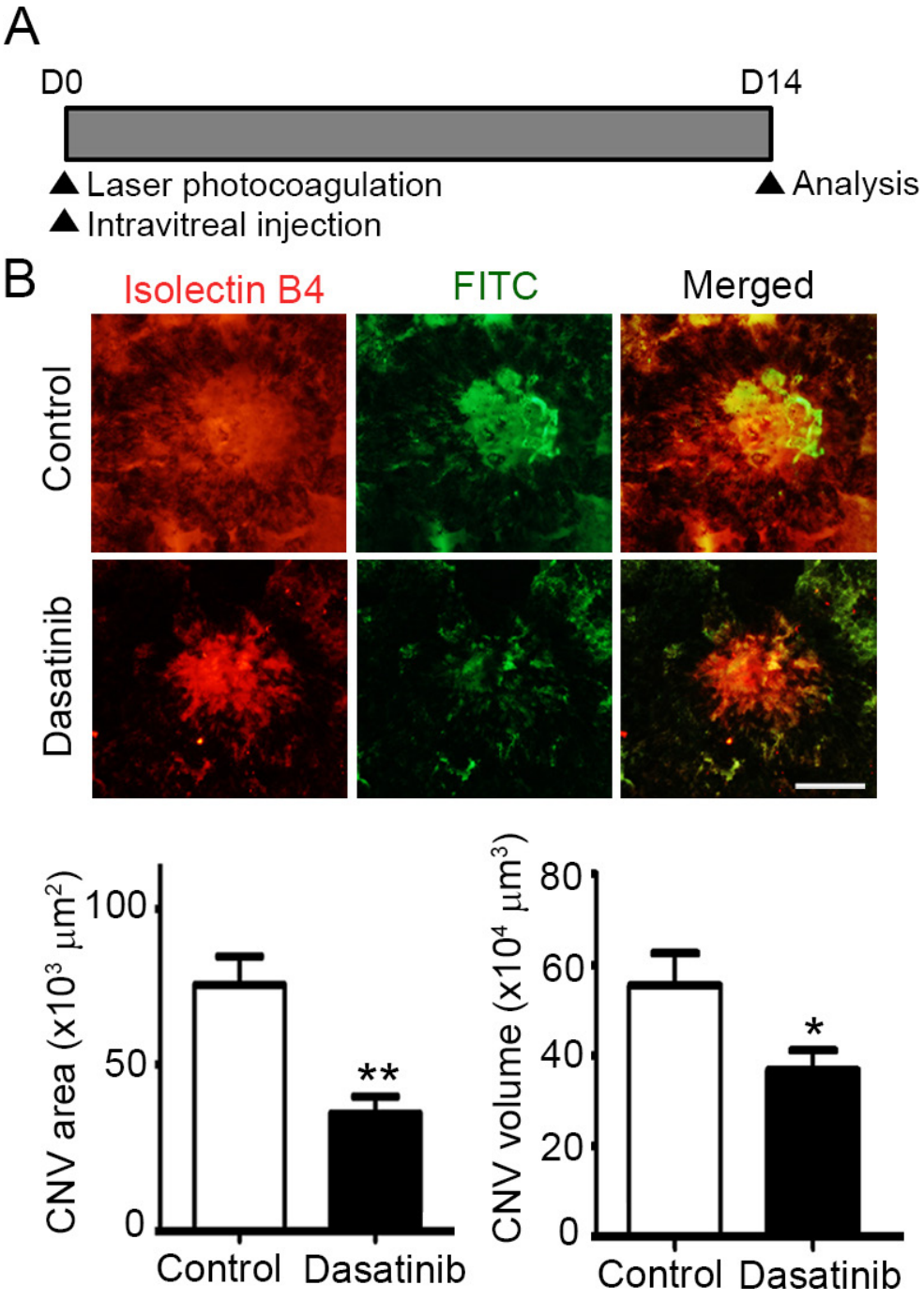

Figure 3. Dasatinib suppresses the development of CNV in a laser-induced mouse model. **A**: Schematic diagram of the laser-induced choroidal neovascularization (CNV) experiment. Immediately after laser photocoagulation, the mice received a single intravitreal injection of dasatinib (1 µg in 1 µl dimethyl sulfoxide [DMSO]) or DMSO (1 µl; contralateral control). Two weeks later, the mice were perfused with fluorescein isothiocyanate (FITC)-labeled dextran (green), and their posterior eyecups comprising the RPE, choroid, and sclera were stained with isolectin B4 (red), an endothelial cell marker. **B**: Representative images of CNV lesions and quantification of the area and volume of the CNV lesions in the mice treated with DMSO (control) or dasatinib. The CNV area was analyzed with measurement of the fluorescence intensity of the images with the isolectin B4–positive area. The CNV volume was calculated as the sum of the CNV areas in confocal Z-stack images. All data are presented as the mean ± standard error of the mean (SEM; *p<0.05, **p<0.01, n=10 mice per group). Scale bar=100 µm.

new vessel growth from the choroid into the subretinal space. Immediately after laser photocoagulation, the mice received a single intravitreal injection of dasatinib or DMSO. Two weeks later, CNV lesions were visualized by perfusing mice with FITC-labeled dextran and staining the choroidal vasculature with isolectin B4 (Figure 3A). Representative images of CNV lesions showed that the dasatinib-treated eyes had significantly less neovascularization than the DMSO-treated control eyes did (Figure 3B). Quantitatively, the area and volume of the CNV lesions in eyes treated with dasatinib were (35.28±5.13) × 10^3 µm² and (36.74±4.43) × 10^4 µm³ (n=10 mice), whereas those in the eyes treated with DMSO were (66.28±5.27) × 10^3 µm² and (55.41±7.16) × 10^4 µm³ (n=10 mice). Compared with that of the DMSO-treated control eyes, the dasatinib-treated eyes had a 46.77% (**p<0.01) and

33.69% reduction (*p<0.05) in the area and volume of the CNV lesions, respectively.

Intravitreal injection of dasatinib does not cause retinal toxicity in mice: To evaluate the retinal toxicity caused by the intravitreal injection of dasatinib in normal mice and in mice with OIR or CNV, we conducted histological examinations and immunohistochemical analyses on ocular tissue sections. The histological examinations of the H&E-stained tissue sections revealed that the dasatinib-injected retinal tissues showed no change in histological morphology or retinal thickness compared with that of the DMSO-injected contralateral eyes (Figure 4A). In addition, GFAP immunohistochemical staining and TUNEL assays revealed that the intravitreal injection of dasatinib into mice with OIR or CNV did not affect GFAP expression and apoptosis levels compared to those observed after DMSO injection (Figures 4B,C). The examination of retinal tissues from normal mice (i.e., without OIR or CNV) also revealed that there were no differences in TUNEL-positive cells and GFAP expression between the dasatinib-treated eyes and DMSO-treated controls (Figure 4B,C). These data suggest that a single intravitreal injection of dasatinib does not cause retinal toxicity in normal mice and in mice with OIR or CNV.

DISCUSSION

Src is a non-receptor tyrosine kinase that interacts with diverse cell-surface receptors and plays a key role in the signal transduction involved in cell growth, differentiation, and migration. In several human tumors, the activities and expression levels of Src are highly elevated, which is known to be important in the promotion of tumor growth and metastasis [12]. In addition to roles in tumor cells, several recent studies have implicated aberrant activation of Src in pathological ocular neovascularization [13-15]. In murine OIR models, Src was highly activated in pathological preretinal vascular tufts and the ganglion cell layer [14]. This increased Src activation

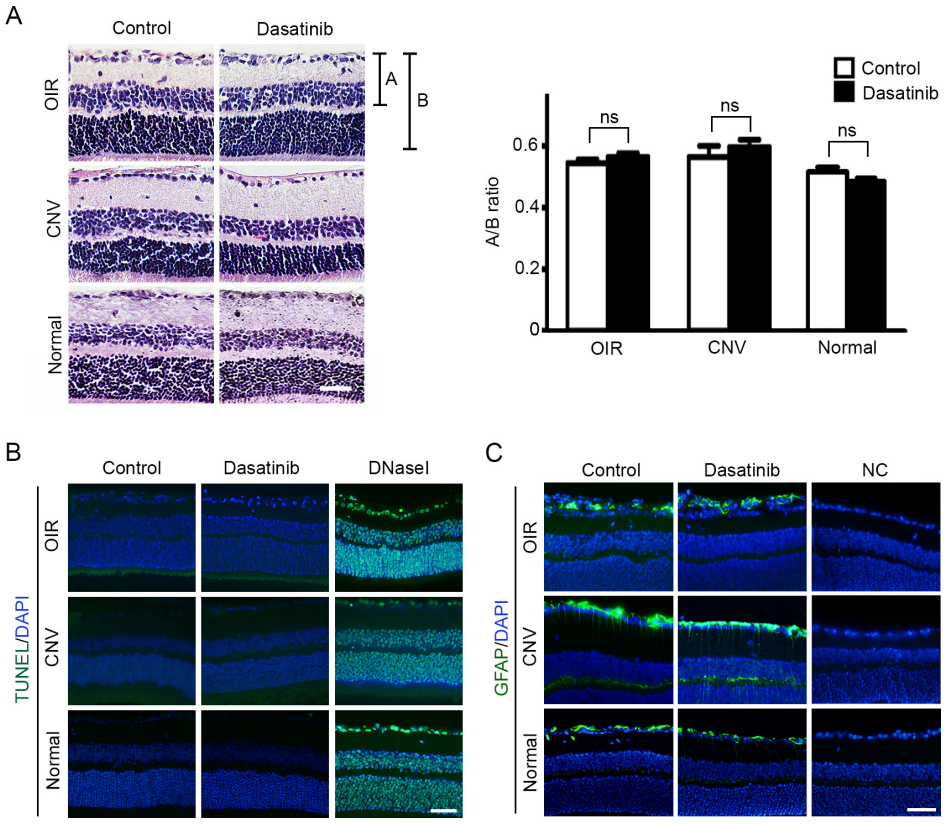

Figure 4. Intravitreal injection of dasatinib does not induce ocular toxicity in mice. Mice received a single intravitreal injection of dasatinib (1 µg in 1 µl dimethyl sulfoxide [DMSO]) or DMSO (1 µl; contralateral control) on P12 (oxygen-induced retinopathy, OIR) or immediately after laser injury (choroidal neovascularization, CNV). On P17 (OIR) or 2 weeks after laser injury (CNV), the eyes were enucleated for histological and immunohistochemical analyses. The retinal toxicity of dasatinib in mice with CNV was assessed in the region without CNV lesions. In addition, normal mice received the same intravitreal administration of dasatinib or DMSO. Two weeks later, the eyes were enucleated for the analysis of retinal toxicity. **A**: Representative images of hematoxylin and eosin (H&E)–stained retinas and quantification of the indicated ratio of A (the distance from the ganglion cell layer to the outer edge of the inner nuclear layer) to B (the distance from the ganglion cell layer to the outer edge of the outer nuclear layer). Data are presented as the mean ± standard error of the mean (SEM; ns=not significant, n=4 mice per group). **B**: Terminal deoxynucleotidyl transferase dUTP nick end labeling (TUNEL) assay and (**C**) immunofluorescence staining with anti-glial fibrillary acidic protein (GFAP) immunoglobulin G (IgG) were performed on tissue sections prepared from the eyecups of mice with OIR or CNV. In (**B**), DNase I-treated sections were included as positive controls. In (**C**), sections stained with nonspecific IgGs were included as negative controls (NC). The nuclei were stained with 4',6-diamidino-2-phenylindole (DAPI; blue). Representative images in (**B**) and (**C**) were selected from four independent experiments with similar results. All scale bars=50 µm.

was abrogated by an intravitreal injection of VEGF-targeted siRNA, which suggests that the hypoxia-induced production of VEGF activated Src in newly forming vasculature [14]. Furthermore, the inhibition of Src expression and activation using siRNA knockdown and chemical inhibitors (e.g., PP2), respectively, significantly reduced the pathological neovascularization in the retina of OIR mice and rats [13,14]. In HRMECs, treatment with siRNA targeting Src, chemical inhibitors, and adenovirus encoding dominant negative form of Src resulted in a significant reduction in VEGF-mediated angiogenic responses [14,15]. These data suggest that Src is an important angiogenic signaling molecule involved in abnormal retinal neovascularization.

Dasatinib was originally developed as a dual inhibitor of Src and BCR/ABL and has been used as an effective therapeutic for imatinib-resistant chronic myelogenous leukemia. Preclinical data have also indicated that dasatinib can inhibit tumor cell growth, migration, and invasion in a variety of solid tumors with elevated expression levels and aberrant activities of Src [16-18]. Recently, it was reported that the anticancer activity of dasatinib was at least partially attributable to its inhibition of VEGF-induced Src activation in endothelial cells [19,20]. In experiments using mouse xenograft models, dasatinib-treated tumor sections exhibited a substantial decrease in Src phosphorylation in tumor-associated endothelial cells compared with that of the vehicle-treated controls [19]. A Matrigel plug assay revealed that dasatinib treatment significantly reduced vascular density in Matrigel plugs containing VEGF [19]. Endothelial cells isolated from patients with multiple myeloma demonstrated that dasatinib suppressed VEGF-induced cell survival, proliferation, migration, and tube formation by inactivating the Src signaling pathway [20]. These data suggest that dasatinib effectively suppresses VEGF-mediated angiogenic responses in tumor-associated endothelial cells. However, the antiangiogenic activity of dasatinib has not been characterized in the context of pathological ocular neovascularization.

In the present study, we examined the inhibitory effect of dasatinib on pathological ocular neovascularization in vitro in HRMECs and in vivo in mouse models of OIR and CNV. Dasatinib treatment inhibited the VEGF-induced angiogenic responses in HRMECs. An intravitreal injection of dasatinib significantly suppressed the neovascularization in retinas of OIR mice and laser-injured choroids of mice. Dasatinib-injected eyes exhibited a substantial decrease in the p-Y416 Src signal in isolectin B4–positive endothelial cells of peri-retinal tufts compared with the signal in DMSO-injected contralateral controls. In addition, the retinal toxicity of dasatinib was evaluated by examining the changes in retinal morphology, GFAP expression, and apoptosis. In the present in vivo experimental setting, a single intravitreal injection of dasatinib did not induce retinal toxicity. These data imply that dasatinib, which has been used to treat chronic myeloid leukemia, may be repositioned as a therapy for the prevention and treatment of pathological ocular neovascularization in patients with ROP, PDR, and neovascular AMD.

ACKNOWLEDGMENTS

This research was supported by National Research Foundation of Korea grant funded by the Korea government [2015R1D1A1A02061724; 2016M3A9A8918381].

REFERENCES

1. Adamis AP, Miller JW, Bernal MT, D'Amico DJ, Folkman J, Yeo TK, Yeo KT. Increased vascular endothelial growth factor levels in the vitreous of eyes with proliferative diabetic retinopathy. Am J Ophthalmol 1994; 118:445-50. [PMID: 7943121].

2. Grisanti S, Tatar O. The role of vascular endothelial growth factor and other endogenous interplayers in age-related macular degeneration. Prog Retin Eye Res 2008; 27:372-90. [PMID: 18621565].

3. Sato T, Kusaka S, Shimojo H, Fujikado T. Vitreous levels of erythropoietin and vascular endothelial growth factor in eyes with retinopathy of prematurity. Ophthalmology 2009; 116:1599-603. [PMID: 19371954].

4. Aiello LP, Avery RL, Arrigg PG, Keyt BA, Jampel HD, Shah ST, Pasquale LR, Thieme H, Iwamoto MA, Park JE, Nguyen HV, Aiello LM, Ferrara N, King GL. Vascular endothelial growth factor in ocular fluid of patients with diabetic retinopathy and other retinal disorder. N Engl J Med 1994; 331:1480-7. [PMID: 7526212].

5. Maguire MG, Martin DF, Ying GS, Jaffe GJ, Daniel E, Grunwald JE, Toth CA, Ferris FL 3rd, Fine SL. Five-Year Outcomes with Anti-Vascular Endothelial Growth Factor Treatment of Neovascular Age-Related Macular Degeneration: The Comparison of Age-Related Macular Degeneration Treatments Trials. Ophthalmology 2016; 123:1751-61. [PMID: 27156698].

6. Talks JS, Lotery AJ, Ghanchi F, Sivaprasad S, Johnston RL, Patel N, McKibbin M, Bailey C, Mahmood S. First-Year Visual Acuity Outcomes of Providing Aflibercept According to the VIEW Study Protocol for Age-Related Macular Degeneration. Ophthalmology 2016; 123:337-43. [PMID: 26578446].

7. Eliceiri BP, Paul R, Schwartzberg PL, Hood JD, Leng J, Cheresh DA. Selective requirement for Src kinases during VEGF-induced angiogenesis and vascular permeability. Mol Cell 1999; 4:915-24. [PMID: 10635317].

8. Abu-Ghazaleh R, Kabir J, Jia H, Lobo M, Zachary I. Src mediates stimulation by vascular endothelial growth factor of the

phosphorylation of focal adhesion kinase at tyrosine 861, and migration and anti-apoptosis in endothelial cells. Biochem J 2001; 360:255-64. [PMID: 11696015].

9. Kim SR, Suh W. Beneficial effects of the Src inhibitor, dasatinib, on breakdown of the blood-retinal barrier. Arch Pharm Res 2017; 40:197-203. [PMID: 27988882].

10. Smith G, McGimpsey WG, Lynch MC, Kochevar IE, Redmond RW. An efficient oxygen independent two-photon photosensitization mechanism. Photochem Photobiol 1994; 59:135-9. [PMID: 8165232].

11. Basavarajappa HD, Sulaiman RS, Qi X, Shetty T, Sheik Pran Babu S, Sishtla KL, Lee B, Quigley J, Alkhairy S, Briggs CM, Gupta K, Tang B, Shadmand M, Grant MB, Boulton ME, Seo SY, Corson TW. Ferrochelatase is a therapeutic target for ocular neovascularization. EMBO Mol Med 2017; 9:786-801. [PMID: 28377496].

12. Summy JM, Gallick GE. Src family kinases in tumor progression and metastasis. Cancer Metastasis Rev 2003; 22:337-58. [PMID: 12884910].

13. Werdich XQ, Penn JS. Specific involvement of SRC family kinase activation in the pathogenesis of retinal neovascularization. Invest Ophthalmol Vis Sci 2006; 47:5047-56. [PMID: 17065526].

14. Zhang Q, Wang D, Kundumani-Sridharan V, Gadiparthi L, Johnson DA, Tigyi GJ, Rao GN. PLD1-dependent PKCgamma activation downstream to Src is essential for the development of pathologic retinal neovascularization. Blood 2010; 116:1377-85. [PMID: 20421451].

15. Toutounchian JJ, Pagadala J, Miller DD, Baudry J, Park F, Chaum E, Yates CR. Novel Small Molecule JP-153 Targets the Src-FAK-Paxillin Signaling Complex to Inhibit VEGF-Induced Retinal Angiogenesis. Mol Pharmacol 2017; 91:1-13. [PMID: 27913654].

16. Trevino JG, Summy JM, Lesslie DP, Parikh NU, Hong DS, Lee FY, Donato NJ, Abbruzzese JL, Baker CH, Gallick GE. Inhibition of SRC expression and activity inhibits tumor progression and metastasis of human pancreatic adenocarcinoma cells in an orthotopic nude mouse model. Am J Pathol 2006; 168:962-72. [PMID: 16507911].

17. Johnson FM, Saigal B, Talpaz M, Donato NJ. Dasatinib (BMS-354825) tyrosine kinase inhibitor suppresses invasion and induces cell cycle arrest and apoptosis of head and neck squamous cell carcinoma and non-small cell lung cancer cells. Clin Cancer Res 2005; 11:6924-32. [PMID: 16203784].

18. Nam S, Kim D, Cheng JQ, Zhang S, Lee JH, Buettner R, Mirosevich J, Lee FY, Jove R. Action of the Src family kinase inhibitor, dasatinib (BMS-354825), on human prostate cancer cells. Cancer Res 2005; 65:9185-9. [PMID: 16230377].

19. Liang W, Kujawski M, Wu J, Lu J, Herrmann A, Loera S, Yen Y, Lee F, Yu H, Wen W, Jove R. Antitumor activity of targeting SRC kinases in endothelial and myeloid cell compartments of the tumor microenvironment. Clin Cancer Res 2010; 16:924-35. [PMID: 20103658].

20. Coluccia AM, Cirulli T, Neri P, Mangieri D, Colanardi MC, Gnoni A, Di Renzo N, Dammacco F, Tassone P, Ribatti D, Gambacorti-Passerini C, Vacca A. Validation of PDGFRbeta and c-Src tyrosine kinases as tumor/vessel targets in patients with multiple myeloma: preclinical efficacy of the novel, orally available inhibitor dasatinib. Blood 2008; 112:1346-56. [PMID: 18524994].

Articles are provided courtesy of Emory University and the Zhongshan Ophthalmic Center, Sun Yat-sen University, P.R. China. The print version of this article was created on 24 November 2017. This reflects all typographical corrections and errata to the article through that date. Details of any changes may be found in the online version of the article.